THE ANNALS OF "DUNAREA DE JOS" UNIVERSITY OF GALATI
FASCICLE IX. METALLURGY AND MATERIALS SCIENCE
N^0. 3 – 2014, ISSN 1453 – 083X

COMPARATIVE CHARACTERISTICS OF MARTENSITE AND BAINITE IN Cu-BASED SMAs

Elena MIHALACHE, Monica-Nicoleta LOHAN, Bogdan PRICOP, Leandru-Gheorghe BUJOREANU, Marius-Gabriel SURU*
Faculty of Materials Science and Engineering, "Gheorghe Asachi" Technical University of Iaşi,
61A Avenue D. Mangeron, 700050 Iaşi, Romania
*Corresponding author
e-mail: marius_suru2005@yahoo.com

ABSTRACT

The present work reports the evolution of micro-structure and shape memory behavior in a Cu-15 Zn-6 Al (mass. %) shape memory alloy (SMA), as a function of the applied hot working procedure and of the performed heat treatments. To this purpose a special compressed-air forging hammer was employed. The samples were heated up to 1023 K into an electric furnace and swaged on a compressed-air forging hammer, by multiple blows. After several blows, the specimens were prepared, by maintaining the main plastic deformation direction, for structural analysis, being cut, embedded, ground, polished and etched. Structural analysis comprised optical (OM) and scanning electron (SEM) microscopy observations, performed with the view of emphasizing the morphological aspects of martensite and bainite. To reveal the atomic fluctuations, enabled by hot forging, energy dispersive X-ray spectroscopy analysis (EDS) measurements were performed by means of SEM analysis. The paper reports the results of OM, SEM and EDS observations, by corroborating the results obtained in martensite and bainite.

KEYWORDS: shape memory alloy, hot forging, martensite, bainite, scanning electron microscopy, atomic fluctuations

1. Introduction

"Shape memory" is the term used to describe a unique property of some materials that undergo the thermoelastic martensitic reaction [1]. It is widely accepted that there are presently five types of commercial shape memory alloys (SMAs): (i) Ni-Ti-based; (ii) Cu-Zn-Al-based [2]; (iii) Cu-Al-Ni-based; (iv) Fe-Mn-Si-based [3] and (v) Fe-Ni-Co-based. Thus, many alloys exhibit shape memory effect (SME) [4], but Ni–Ti-based shape memory alloys have up to date provided the best combination of materials properties for most commercial applications. Cu-based SMAs [5] are the most promising in practical use because of their low price, high recovery force and because they provide a more economical alternative to Ni–Ti SMAs. Cu–Zn–Al alloys are now the most popular Cu-based SMAs and presently available on the market [6]. However they exhibit poor ductility problems, martensitic stability and intergranular crack, which are disadvantages to their applications [7].

The so-called SME in copper-based alloys is intrinsically related to the martensitic transformation which occurs from the austenite phase (β) [8] to the martensite (β') [9]. Specifically, in Cu–Zn–Al alloys [10], the SME [11] is only observed for a certain range of composition [12] which in general contains Cu–(16–30)Zn–(4–8)Al (wt.%) [13]. With respect to this compositional range, three equilibrium phases (α, β and γ) [14] may occur as well as their respective martensitic ones, typically denoted as α', β' and γ' [15]. The only phase that presents the SME is the β one. The β-phase in Cu–Zn–Al alloys is disordered at high temperatures and has a bcc lattice. During the cooling process, the parent β-phase may give rise to two different superlattice structures, depending on the temperature and alloy composition, by means of an ordering reaction. These structures are normally designated as β_2 (B2) and β_3 ($L2_1$). By stress-induced or thermally [16], the β_2 or β_3 austenite phases are transformed into the β' one (martensite) which is also known as 9R [17] due to the rhombohedral lattice and stacking of 9 compact plans.

In contrast to martensite transformation, bainite transformation [18] is of diffusion-controlled type because no intermediate, transition lattice was observed even in the very tip of the bainite plate. After several decades of intensive fundamental research of bainite transformation in steels [19], various issues are still not fully understood such as bainite formation from plastically deformed austenite and its large growth rate and autocatalytic nucleation [20]. The purpose here has been to emphasize the comparative morphological aspects of martensite and bainite as a function of the applied hot working procedure and of the performed heat treatments.

2. Experimental procedure

A conventional SMA with nominal chemical composition Cu-15 Zn-6 Al (mass %) was melt in an induction furnace, cast and normalized. From the obtained specimens, 5×10^{-3} m-thick samples were cut in order to be plastically deformed by hot forging. The plastic deformation process consisted in repetitive forging of billets transversally cut from cylindrical ingots.

The billets were heated up to 1023 K, into an electric furnace and swaged on a compressed-air forging hammer, by multiple blows until sample's thickness was reduced from 5 to 2×10^{-3} m. From repeatedly hot forged samples, different specimens were homogenized at 1073 K, tempered at 573 and 673 K and finally cooled in water [21].

For structural analysis, the specimens were cut, embedded, ground, polished and etched. Embedding was performed into bi-component cold mounting resin. Grinding was done with abrasive paper with meshes raging between 600 and 2400, under intense water cooling, in order not to affect the thermomechanical history of the specimens. Polishing was achieved in two stages.

Firstly the specimens were manually polished with 6 μm diamond paste and then were automatically polished with 0.3 μm and finally with 0.04 μm alumina powder solution, diluted in a ratio of 1:10. Chemical etching, which is essential for a proper visualization of surface structure [20] was carried out with 30% HNO_3 in 100 ml aqueous solution.

Comparative structural analysis comprised optical (OM), scanning electron microscopy (SEM) and energy dispersive X-ray spectroscopy analysis (EDS), performed with the aiming to emphasize the micro-structural effects, of the above mentioned plastic deformation process and the performed heat treatments, on martensite and bainite plate morphology. OM micrographs were recorded with an OPTIKA XDS-3 MET microscope equipped with OPTIKAM 4083.B5 microscopy digital USB camera and OPTIKAM B5 software. SEM and EDS analyses were recorded using a SEM—VEGA II LSH TESCAN microscope, coupled with an EDX—QUANTAX QX2 ROENTEC detector.

3. Results and discussions

The first series of OM micrographs, revealing general aspects concerning the effects of the hot forging and of the performed heat treatments, are summarized in Fig. 1 The representative detailed aspects of martensite plates of specimens tempered at 573 K are illustrated in Fig. 1(b). The micrographs represent a martensitic type structure (M) with a Zig-Zag morphology. One can, observe on the corners of the plates, the central ribs corresponding to the first twining plan. The variations of martensite plates (V1 and V2) with different contrast (light-dark) are symmetrically disposed to the central midrib. The primary martensite plates can be distinguished easily thanks to their micrometric dimension and the secondary plates are thinner, being disposed within primary ones.

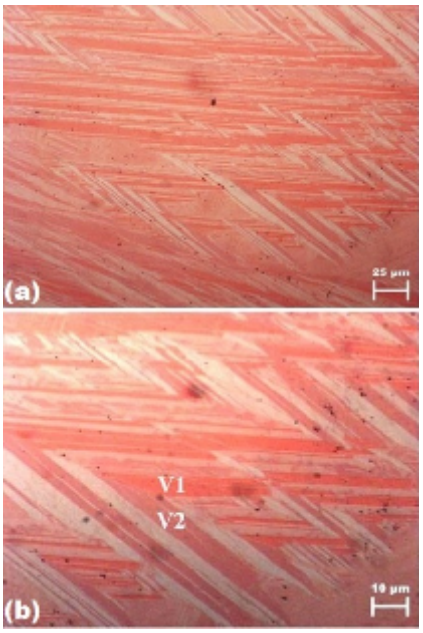

Fig. 1. *OM micrographs of specimens tempered at 573 K (a) general aspect; (b) detailed aspect of martensite plates on the surface of specimens*

The martensite plate variants V1 and V2, which are in the twining relation, together with the presence of central midrib, are characteristic features to the diamond-type structure. In the detwining area the presence of austenite (A) can be observed.

The displacement mode of the bainite lamellar structure on the surface of the specimens is summarized in Fig. 2. In the optical micrographs from Figures. 2(a) and (b) the parallel disposal of bainite plates and their submicron thickness can observed.

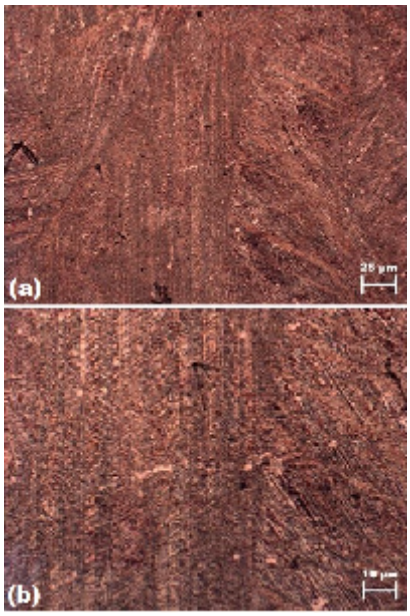

Fig. 2. *OM micrographs of specimens tempered at 673 K (a) general aspect; (b) detail of bainite lamellar structure, illustrating their displacement mode on the surface of the sample*

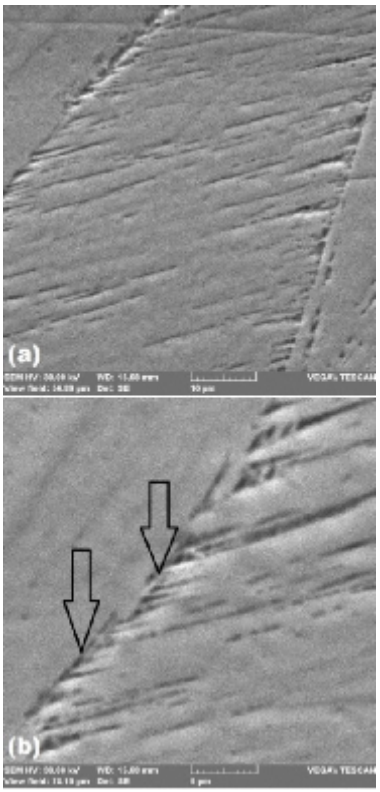

Fig. 3. *Characteristic SEM micrographs of specimens tempered at 573 K (a) general aspect; (b) detail of martensite plates with localization of central midrib*

Figure 3 provides details, by means of SEM micrographs, of martensite plates on the same specimens as Fig. 1. The SEM micrographs are showing parallel and relatively small depth martensite plates. On the micrograph it was marked through a double arrow the position of the central rib, identified in Fig. 1. Thus, the substructure of martensite plates can be observed at higher power magnification, such as Fig. 3(b), where it can be seen that the martensite plates have the thickness order of 10 μm, and the subplates the order of 2-3 μm.

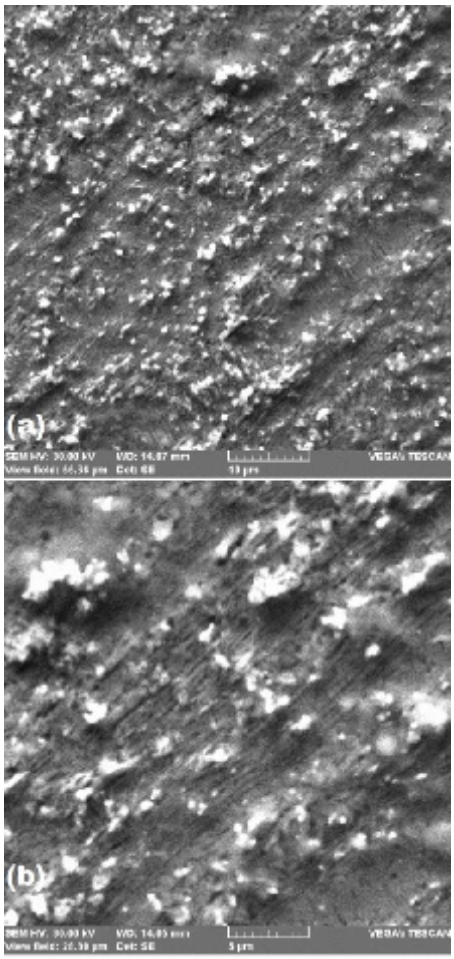

Fig. 4. *Characteristic SEM micrographs of specimens tempered at 673 K (a) general aspect; (b) detail of bainite structure*

A series of additional morphological details are noticeable in Fig. 4, on the same specimens used in Fig. 2. Knowing that bainite features include the platiform aspects, the presence of internal ribs, distributed irregularly and having micro-twining aspect, it can be said that the structure in Fig. 4 belongs to bainite. The internal ribs are so fine that they cannot be observed only at a higher power magnification, such as the example in Fig. 4(b).

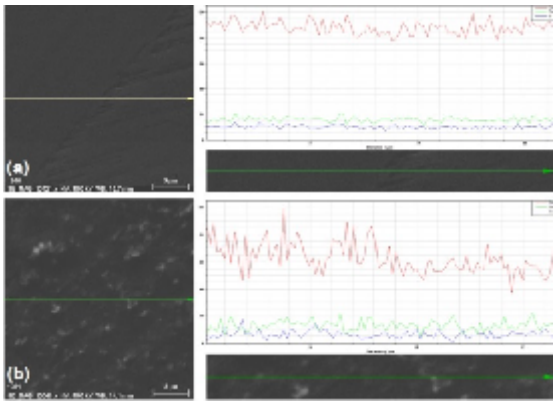

Fig. 5. *Typical EDS analysis illustrating the position of composition line and corresponding atomic fluctuations: (a) martensite (573 K tempering); (b) bainite (tempering 673 K)*

To emphasize the controlled character by diffusion of bainite growth, it was made EDS analysis, aiming at the difference between martensite and bainite, the results are presented in Fig. 5. The results show clearly that between martensite and bainite there is a significant atomic migration. As the martensitic transformation is diffusion free, the one that could produce atomic movement from the equilibrium positions is the increase of bainite that is produced by diffusion.

The chemical composition fluctuations from Fig. 5(a), corresponding to martensite, have cca. 40% at. on Cu and aprox 10% at. on Zn and Al. In contrast with these values, the bainite specimens were max 20% at. on Cu, respectively 5% at. on Zn and Al.

4. Conclusions

In this paper the morphological, mechanical and structural main features of martensite and bainite were presented. In this way a bibliographic synthesis, including the historical evolution, the characteristics and development prospects of bainite steels were developed.

Based on the platiform character printed by plates with irregular internal ribs with micro-twin aspect and the controlled increase of bainite, has been identified his present in CuZnAl shape memory alloy, homogenized and tempered at 673 K.

By means of optical and electronic microscopy was revealed a clear differentiation between bainitic and martensitic structures. With the aid of X - ray dispersion analysis (EDS), the study highlighted the atomic fluctuation increase, which assigned the bainite difussional carachter, as follows: on martensite (tempering 573 K) Cu fluctuated by max 20% at., and on bainite (tempering 673 K) fluctuated aprox. 40% at. Similarly at Zn and Al fluctuated by aprox. 10% at. on bainite.

Acknowledgement

For this research the authors are pleased to acknowledge the financial support of UEFISCDI by means of the project PN-II-ID-PCE-2012-4-0033, contract 13/2013.

References

[1]. C. Y. Chung, C. W. H. Lam - *Cu-based shape memory alloys with enhanced thermal stability and mechanical properties*, Materials Science and Engineering: A, 273–275, 1999, p. 622-624.
[2]. M.-G. Suru, C. Moroşanu, L.-G. Bujoreanu - *Variation tendencies of shape memory alloys surface relief as a function of training-cycling parameters*, Journal of optoelectronics and advanced materials, 16, 2014, p. 394 – 400.
[3]. M.-G. Suru, I. Dan, N. M. Lohan, A. L. Paraschiv, B. Pricop, I. P. Spiridon, C. Baciu, L.-G. Bujoreanu - *Effects of hot working procedure on surface relief characteristic in an Fe–Mn–Si–Cr shape memory alloy*, Mat.-wiss. u. Werkstofftech., 45, 2014, p. 44-50.
[4]. H. LIU, N. SI, G. XU - *Influence of process factors on shape memory effect of CuZnAl alloys*, Transactions of Nonferrous Metals Society of China, 16, 2006, p. 1402-1409.
[5]. J. Fernandez, X. M. Zhang, J. M. Guilemany - *A one-cycle training technique for copper-based shape memory alloys*, Journal of Materials Processing Technology, 139, 2003, p. 117-119.
[6]. C. E. Sobrero, P. La Roca, A. Roatta, R. E. Bolmaro, J. Malarría - *Shape memory properties of highly textured Cu–Al–Ni–(Ti) alloys*, Materials Science and Engineering: A, 536, 2012, p. 207-215.
[7]. J. M. Jani, M. Leary, A. Subic, M. A. Gibson - *A review of shape memory alloy research, applications and opportunities*, Materials & Design, 56, 2014, p. 1078-1113.
[8]. L.-G. Bujoreanu - *On the influence of austenitization on the morphology of α-phase in tempered Cu–Zn–Al shape memory alloys*, Materials Science and Engineering A, 481–482, 2008, p. 395–403.
[9]. R. S. Elliott, D. S. Karls - *Entropic stabilization of austenite in shape memory alloys*, Journal of the Mechanics and Physics of Solids, 61, 2013, p. 2522-2536.
[10]. M.-G. Suru, A.-L. Paraschiv, N. M. Lohan, B. Pricop, B. Ozkal, L.-G. Bujoreanu - *Loading Mode and Environment Effects on Surface Profile Characteristics of Martensite Plates in Cu-Based SMAs*, Journal of Materials Engineering and Performance, online first, DOI: 10.1007/s11665-014-0951-6.
[11]. M.-G. Suru, L.-G. Bujoreanu - *Comparative topographic study of surface micro-relief of primary martensite plates in shape memory alloys with different crystalline structures*, Mat.-wiss. u.Werkstofftech, 43, 2012, p. 973-978.
[12]. M. Blanco, J. T. C. Barragan, N. Barelli, R. D. Noce, C. S. Fugivara, J. Fernández, A. V. Benedetti - *On the electrochemical behavior of Cu–16%Zn–6.5%Al alloy containing the β'-phase (martensite) in borate buffer*, Electrochimica Acta, 107, 2013, p. 238-247.
[13]. J. X. Zhang, Y. X. Liu, W. Cai, L. C. Zhao - *The mechanisms of two way-shape memory effect in a Cu-Zn-Al alloy*, Materials Letters, 33, 1997, p. 211-214.
[14]. R. Abeyaratne, J. K. Knowles - *On the kinetics of an austenite → martensite phase transformation induced by impact in a Cu-Al-Ni shape-memory alloy*, Acta Materialia, 45, 1997, p. 1671-1683.
[15]. A. M. Furlani, M. Stipcich, R. Romero - *Phase decomposition in a β Cu–Zn–Al–Ti–B shape memory alloy*, Materials Science and Engineering: A, 392, 2005, p. 386-393.

[16]. N. F. Kennon, D. P. Dunne - *Shape strains associated with thermally-induced and stress-induced martensite in a Cu-Al-Ni shape memory alloy*, Acta Metallurgica, 30, 1982, p. 429-435.
[17]. M. G. Suru, A. L. Paraschiv, B. Pricop, L. G. Bujoreanu - *A statistical evaluation of thermomechanical loading effects on martensite plate morphology in CuZnAl SMAs*, Optoelectronics and advanced materials – rapid communications, 7, 2013, p. 141 – 144.
[18]. L. G. Bujoreanu, S. Stanciu, P. Bârsănescu, N. M. Lohan - *Study of the transitory formation of α1 bainite, as a precursor of α-phase in tempered SMAs*, Proc. of SPIE, 7297, 2009, 72970B-1-5.
[19]. G. Sidhu, S. D. Bhole, D. L. Chen, E. Essadiqi - *An improved model for bainite formation at isothermal temperatures*, Scripta Materialia, 64, 2011, p. 73-76.
[20]. O. Bouaziz, P. Maugis, J. D. Embury - *Bainite tip radius prediction by analogy with indentation,* Scripta Materialia, 54, 2006, p. 1527–1529.
[21]. G. Vitel, A. L. Paraschiv, M. G. Suru, N. Cimpoeşu, L.-G. Bujoreanu - *Tempering effects in a normalized hot forged Cu-Zn-Al shape memory alloy*, Optoelectronics and advanced materials – rapid communications, 6, 2012, p. 339-342.